

TERAHERTZ RADIATION

PACS numbers: 78.45.+h; 42.55.Px; 71.55.Eq; 42.55.Lt
DOI: 10.1070/QE2015v045n02ABEH015530

Stimulated emission on impurity–band optical transitions in semiconductors

N.A. Bekin, V.N. Shastin

Abstract. **This paper examines conditions for population inversion and amplification in the terahertz range using impurity–band electron transitions in semiconductors and semiconductor structures. Our estimates indicate that stimulated emission on such transitions under optical excitation of impurities can be obtained in a semiconductor with a sufficiently high doping level if electron heating is restricted. At a CO_2 laser pump power density near 0.2 MW cm^{-2} (photon energy of 117 meV), the gain in n-GaAs may exceed the loss by 50 cm^{-1} provided the electron gas temperature does not exceed 40 K. We analyse the influence of the carrier effective mass and doping compensation on the gain coefficient and briefly discuss the use of resonance tunnelling for obtaining stimulated emission on impurity–band transitions in quantum cascade heterostructures.**

Keywords: *laser, population inversion, shallow impurities, quantum wells, impurity–band optical transitions.*

1. Introduction

The frequency range of typical optical transitions related to states of shallow impurity centres (donors and acceptors) in semiconductors is 1–10 THz, and this cannot but be of interest for developing novel terahertz radiation sources. Having a wide application area, such sources are now receiving a great deal of attention.

Most effort has been concentrated on improving quantum cascade schemes operating on electronic transitions between size-quantised 2D subbands [1]. At the same time, studies examining the use of shallow impurity centres have emerged comparatively recently and deal primarily with silicon. The results obtained to date demonstrate the possibility of stimulated emission on $2p_0 - 1s$ and $2p_\pm - 1s$ intracentre transitions of optically excited group V donors (P, Sb, As, Bi) in silicon [2]. Adam et al. [3] and Lv et al. [4, 5] investigated the characteristics of spontaneous THz emission from boron and gallium acceptors and phosphorus donors in silicon under electric breakdown conditions. Shalygin et al. [6] discovered and studied THz electroluminescence of silicon and oxygen donors in GaN. Note that it corresponds to both intracentre and impurity–band optical transitions. The photoluminescence spectrum of donors in GaAs:Si under interband excitation also corresponds to intracentre and impurity–band transitions [7].

The purpose of this work is to theoretically assess the feasibility of stimulated emission on impurity–band optical transitions, i.e. on transitions of charge carriers from a continuum of states (CS) to the ground state (GS) of a donor or acceptor (Fig. 1). Such a medium would be expected to have a broad gain band and a gain coefficient that is a weak function of the concentration broadening of working states due to the influence of some impurity centres on the energy of others. Note that such broadening suppresses stimulated emission on intracentre transitions of donors in silicon even at dopant concentrations of $\sim 10^{16}$ cm^{-3} [8] and limits the gain coefficient to a level of 2–3 cm^{-1}. The use of CS–GS transitions might ensure a larger gain coefficient owing to a higher dopant concentration. An important role is, however, played by the parameters and specifics of the semiconductor. For example, as shown below, a three-level gain on impurity–band transitions is difficult to realise in bulk n-Si, because it requires too high an excitation power in the case

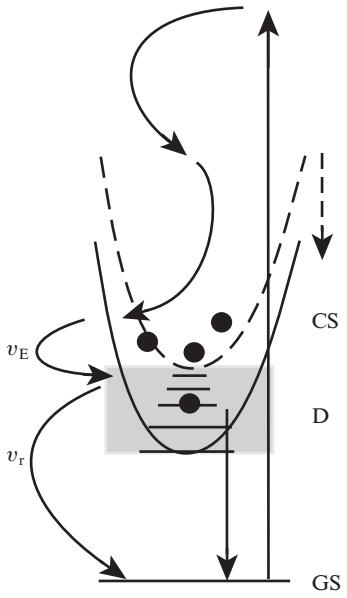

Figure 1. Energy band diagram in the case of an increased doping level and schematic of inverted distribution formation on impurity–band optical transitions. The grey region represents the energies of quasi-localised states. The vertical arrows represent pumping-induced optical transitions (upwards) and emission on working transitions (downwards), and the curved arrows represent relaxation processes through the emission of optical and acoustic phonons.

N.A. Bekin, V.N. Shastin Institute for Physics of Microstructures, Russian Academy of Sciences, Akademicheskaya ul. 7, 607680 der. Afonino, Kstovskii raion, Nizhnii Novgorod region, Russia; e-mail: nbekin@ipm.sci-nnov.ru, shastin@ipm.sci-nnov.ru

Received 11 April 2014
Kvantovaya Elektronika **45** (2) 105–112 (2015)
Translated by O.M. Tsarev

of optical pumping. On the other hand, in the case of n-GaAs doped to $\sim 10^{16}$ cm^{-3} a gain coefficient of ~ 100 cm^{-1} might be expected, which makes a laser based on impurity–band transitions conceptually feasible, in particular in size-quantised heterostructures under both optical [9] and, possibly, electrical [10, 11] pumping.

The idea of light emission on CS–GS transitions was first suggested in 1959 [12]. It was assumed that a higher population of continuum states in comparison with the population of the states of Coulomb centres (inverse population) – a necessary condition for electromagnetic wave amplification – could be obtained through their breakdown by an electric field pulse. The idea, however, has not been elaborated on, which is not surprising in view of the concomitant problems. Note, first of all, the problem of producing an inverse population of working states. The breakdown of impurity centres is accompanied by considerable carrier heating, which prevents the formation of a required distribution. However, impossible under breakdown conditions, inverse populations can be produced by electrical pumping. For example, this can be achieved in the case of vertical transport through a 2D quantum cascade in heterostructures owing to phonon-assisted resonance tunnelling [10]. Moreover, the problem of inverse population of states on impurity–band transitions can be resolved via the optical ionisation of impurity centres. Carrier heating can readily be minimised by adjusting the pump wavelength. This approach is effective for both bulk semiconductors and semiconductor structures. There is, however, another serious obstacle: absorption by continuum electrons. It should also be taken into account that a considerable fraction of such electrons are localised to some extent at the Coulomb potential of Coulomb centres or their complexes, and such absorption is difficult to analyse theoretically.

Section 2 discusses conditions for an inverse population and gain on CS–GS transitions under optical excitation, and Section 3 presents an estimate of the relationship between the gain and absorption cross sections and formulates conditions for stimulated emission. Section 4 discusses the obtained results and addresses the problem of replacing optical pumping by electrical injection in quantum cascade heterostructures. The last section formulates the principal conclusions stemming from the present results.

2. Population and gain on working transitions

For simplicity, we will restrict our consideration to donors under optical excitation and make estimates using a number of assumptions and simplifying ideas and comparing three- and two-dimensional systems. We are interested in doping levels from 10^{16} to 10^{17} cm^{-3} for n-GaAs and from 10^{17} to 10^{18} cm^{-3} for n-Si. At these dopant concentrations, the $2p_0$, 2s, $2p_\pm$ and other excited states of the donor form a band of quasi-localised states, D, which 'transforms' into a continuum of free carriers, CS (Fig. 1). Note that, being inhomogeneously broadened, the 1s ground state remains localised (cf. Ref. [13]). A corresponding analysis of the density of states of phosphorus donors in silicon was presented by Altermatt et al. [13]. Here we will restrict our consideration to a three-level system in which the ground state (GS) of the centre, being the lower state of the working transition, is depopulated by optical pumping. As a result, electrons pass to continuum states, which is followed by fast ($\sim 10^{12}$ s^{-1}) emission of optical phonons. At a favourable relationship between the pump photon and optical phonon energies (Fig. 1), most of the excited charge carriers relax to the bottom of the D band, to a narrow energy range, and their distribution function is determined by the ratio of their recombination rate v_r (capture in the ground state) to the rate of energy relaxation (thermalisation) through acoustic phonon emission, v_E [14]. Most importantly, we assume that Auger recombination [14] through collisions in the D band is suppressed owing to carrier localisation, inherent in this region. Thus, it is reasonable to expect that the recombination rate is close to the rate of acoustic phonon-mediated thermalisation ($v_r \leqslant v_E$) and is a weak function of the concentration of charged Coulomb centres (cf. Ref. [15]). It is also reasonable to assume that the continuum electrons (including region D) follow Boltzmann statistics and that the effective electron temperature T_e can be estimated from a balance equation. The electron distribution over the 3D continuum states then has the form

$$f_{3D}(E) = \frac{n_{3D}}{\eta N_c}\exp\left(-\frac{E}{k_B T_e}\right), \tag{1}$$

where n_{3D} is the continuum electron concentration; $N_c = 2 \times [mk_B T_e/(2\pi\hbar^2)]^{3/2}$ is the effective density of states; η is the number of equivalent minima in the Brillouin zone; and E is energy, measured from the D band bottom. For simplicity, the density of states near a minimum is taken to vary with energy in the same manner as in the case of a parabolic band. The electron concentration in the continuum is given by

$$n_{3D} = \frac{N^0_{3D} v_I^{(3D)}}{v_r^{(3D)}} = \frac{N^0_{3D} \sigma_I^{(3D)} F}{v_r^{(3D)}},$$

where $v_I^{(3D)}$ and $\sigma_I^{(3D)}$ are the photoionisation rate and cross section, respectively; N^0_{3D} is the concentration of neutral impurity centres; and F (photon cm^{-2} s^{-1}) is the pump photon flux density. The parameters N, n, σ and v depend on the dimensionality of the system, but we will omit the subscript 3D or 2D when this cannot cause confusion.

Similarly, taking into account the changes produced in the photoionisation cross section, recombination rate and other parameters by the decrease in dimensionality, we can consider a 2D system. The electron distribution over 2D continuum states has the form

$$f_{2D}(E) = \frac{\pi\hbar^2 n_{2D}}{\eta m k_B T_e}\exp\left(-\frac{E}{k_B T_e}\right), \tag{2}$$

where $n_{2D} = N_{2D}\sigma_I^{(2D)} F/v_r^{(2D)}$ is the two-dimensional electron concentration in the continuum at a two-dimensional dopant concentration N_{2D}.

The population of the ground state is then

$$f_{GS} = \frac{N^0}{N} = \frac{1-K}{1+v_I/v_r}, \tag{3}$$

where N is the total concentration of major doping centres corresponding to the dimensionality of the system and K is the compensation ratio. Note that $N = N^0 + N^+$, where $N^+ = KN + n$ is the charged centre concentration. Therefore, the condition for inverse population and gain in terms of continuum occupation numbers has the form

$$f = \frac{v_I(1-K)}{(v_I+v_r)d} > \frac{1-K}{1+K+2v_I/v_r}, \tag{4}$$

where d in the case of band bottom states in 3D and subband bottom states in 2D is given by

$$d_{3D} = \frac{2\eta}{N_{3D}}\left(\frac{mk_B T_e}{2\pi\hbar^2}\right)^{3/2},$$

$$d_{2D} = \frac{\eta m k_B T_e}{\pi\hbar^2 N_{2D}}.$$

Since Boltzmann statistics is assumed to be obeyed, we have $d > 1$. From (4), we have for the threshold excitation rate $v_I = v_{th}$:

$$\frac{v_{th}}{v_r} = \frac{1}{4}\left[d - 1 - K + \sqrt{(d-1-K)^2 + 8d}\right]. \quad (5)$$

The gain/absorption coefficient for the working transition can also be obtained readily:

$$\alpha(\omega) = \sigma_I(\omega)[2N^+ f - N^0(1-f)], \quad (6)$$

where $\sigma_I(\omega)$ is the frequency-dependent photoionisation cross section. The additional factor 2 in (6) in front of the term corresponding to emission is due to the double spin degeneracy of the ground state level of an ionised centre. The maximum cross section σ_I is essentially independent of donor concentration [16]. In Si : P, it is near 10^{-15} cm^2 at a frequency $\nu = \omega/(2\pi)$ $\approx$ 10 THz (40 meV) [16]; in n-GaAs, according to calculations it is 6×10^{-14} cm^2 at $\nu \approx 1.5$ THz (6 meV). An expression for the photoionisation cross section is given below.

In the 2D case, one should use volume concentrations in (6): $N^0 = N^0_{2D}/L$ and $N^+ = N^+_{2D}/L$, where L is the quantum well width or superlattice period.

The photoionisation cross section σ_I in Eqn (6) depends on the dimensionality of the system. Consider first a 3D system. In the approximation of hydrogen-like wave functions of a 3D continuum, σ_I has the form [17]

$$\sigma_I^{(3D)}(\omega) = \frac{2^9\alpha\pi^2 a^2}{3\sqrt{\varepsilon}}\left(\frac{E_i}{\hbar\omega}\right)^4 \frac{\exp[-4\arctan(\theta)/\theta]}{1-\exp(-2\pi/\theta)}, \quad (7)$$

where $\alpha = q^2/\hbar c$ is the fine-structure constant; q is the electron charge; c is the speed of light; $\theta = \sqrt{\hbar\omega/E_i - 1}$; $E_i = mq^4 \times (2\varepsilon^2\hbar^2)^{-1}$is the binding energy; ε is the relative dielectric permittivity; and $a = \varepsilon\hbar^2/(mq^2)$ is the Bohr radius. We neglect effective mass (m) anisotropy. In this approach, photoionisation has a maximum at the red limit of the photoeffect.

Using matrix elements for optical transitions between the ground state and continuum states of a two-dimensional hydrogen atom [18], we can find the 2D photoionisation cross section:

$$\sigma_I^{(2D)}(\omega) = \frac{8\alpha\pi^2 a^2}{\sqrt{\varepsilon}}\left(\frac{E_i}{\hbar\omega}\right)^3 \frac{\exp[-2\arctan(\theta)/\theta]}{1+\exp(-\pi/\theta)}, \quad (8)$$

where all notations are the same as in (7). The Bohr radius remains the same, and the binding energy increases four times: $E_i = 2mq^4/(\varepsilon^2\hbar^2)$.

It follows from (4) and (5) that the threshold excitation rate decreases with increasing K, but the effect is rather weak. For example, at $T_e = 40$ K the v_{th}/v_r ratio in gallium arsenide decreases from 1.35 at $K = 0$ to 1.2 at $K = 0.5$. Note that v_r is also a weak function of compensation [15].

The threshold condition (5) is too mild for lasing, because it is necessary to obviate electrodynamic losses, in particular, Drude losses (see Section 3). In connection with this, compensation may have a negative effect. First, compensation increases the Drude absorption because of the increase in the concentration of scattering ionised centres. Second, starting at a certain threshold [above (5)], high excitation rates lead to a decrease in gain coefficient (6) with increasing K. This is related to the adverse effect of compensation on the electron distribution in the continuum [$f \propto v_I(1-K)$, see (4)]. Given the above, in what follows we consider uncompensated semiconductors.

To estimate the threshold photoionisation power, we use the photoionisation cross section σ_I (7). If a CO_2 laser is used as a pump source, the photoionisation cross section in n-GaAs is $\sigma_I = 8 \times 10^{-18}$ cm^2 ($\hbar\Omega = 117$ meV). Note that the photoionisation cross section estimated for the collision mechanism using the Drude classical formula (collision frequency of $\sim 10^{12}$ s^{-1}) is $\sigma_I \sim 10^{-17}$ cm^2. This means that the threshold excitation powers given below for n-GaAs are actually lower by about a factor of 2.

To estimate the ground state recombination rate v_r, we use the following model: The most likely transition is that from the bottom of the D band to the ground state. The band bottom corresponds to the lower excited state energy in the isolated Coulomb centre approximation. Using this approximation, we take v_r to equal the probability of the electron transition from the $2p_0$ state to the ground state via the emission of an acoustic phonon. If the crystal temperature is low enough, we can limit ourselves to spontaneous processes. Then, taking into account the large energy difference of the transition ($\Delta E/\hbar s \gg a^{-1}$, where s is the speed of sound), we have [14]

$$v_r = \frac{2^{19} E_D^2 m^3 s^3 \varepsilon^2}{3^5\pi\hbar^2 q^4 \rho_{cr}}, \quad (9)$$

where E_D is the deformation potential and ρ_{cr} is the density of the crystal.

For shallow donors in GaAs, $v_r = 2 \times 10^6$ s^{-1}. For comparison, in a model proposed by Abakumov et al. [15] the excited-state (D band) capture rate v_c is 3×10^7 s^{-1} ($N_{3D} = 10^{16}$ cm^{-3}). Note that v_c is independent of the lattice and electron temperatures. If Auger processes play a significant role in ground-state nonradiative recombination, the recombination rate may be comparable to the capture rate: $v_r \leqslant v_c$. In the case of the upper estimate, $v_r \approx v_c \approx 3 \times 10^7$ s^{-1}, the threshold power density ($v_{th}/v_r \approx 1.3$, $T_e = 40$ K) is 0.1 MW cm^{-2}. However, as mentioned above, Auger processes are suppressed because of the partial electron localisation in the D band, so the recombination rate should be lower, which would lead to a reduction in threshold power density. The threshold power density decreases as well with decreasing pump photon energy $\hbar\Omega$: at $\hbar\Omega = 50$ meV ($\sigma_I \approx 10^{-16}$ cm^2) and $v_r \approx 3 \times 10^7$ s^{-1}, it is 3 kW cm^{-2}.

In the effective mass approximation ($m = 0.32m_0$, where m_0 is the free-electron mass), we obtain for n-Si $\sigma_I \approx 5 \times 10^{-17}$ cm^2 ($\hbar\Omega = 117$ meV). In the above model [15], the excited-state capture rate is rather high: $v_c = 5 \times 10^{10}$ s^{-1} at $N_{3D} = 3 \times 10^{17}$ cm^{-3}. Given that the donor binding energy in silicon ($\sim$40 meV) is substantially higher than that in n-GaAs, the ground state recombination rate would be expected to be several times lower than the above excited-state capture rate. Then, taking $v_r \approx 10^{10}$ s^{-1}, we obtain that the threshold power density is 10 MW cm^{-2} ($v_{th}/v_r \approx 2.6$, $T_e = 40$ K). A negative role is played not only by the high recombination rate in n-Si

but also by the sixfold degeneracy of the valleys ($\eta = 6$), which leads to the corresponding reduction in the occupation numbers (1). By reducing the pump photon energy to 50 meV ($\sigma_I \approx 6 \times 10^{-16}$ cm^2), the threshold power density can be lowered to 0.4 MW cm^{-2}. Lowering the electron temperature to 20 K will reduce the v_{th}/v_r ratio by almost a factor of 3. Given that v_r is a weak function of temperature, lowering the electron temperature clearly allows the threshold pump power to be reduced.

Electron recombination to the ground state of impurities in quantum wells can be considered in a similar manner. To this end, we estimate, in a one-centre approximation, the probability of an electron transition from the $2p_0$ state – with the corresponding level thought of as the bottom of the D band – to the 1s ground state. In the quasi-two-dimensional approximation, where the energy difference between lower subbands considerably exceeds the impurity binding energy, the wave functions of the impurity states can be written as the product of functions of ρ and z: $\psi_{1s} \approx \beta_1 \exp(-\beta_1\rho/2)\psi_1(z) \times (\sqrt{2\pi})^{-1}$ and $\psi_{2p_0} \approx \beta_2(1 - \beta_2\rho)\exp(-\beta_2\rho/2)\psi_1(z)/\sqrt{6\pi}$, where $\psi_1(z)$ is the wave function of the lower subband. For the lateral degrees of freedom, we used the form of the wave function of a two-dimensional hydrogen atom [18]. To take into account the variation in energy and the length scale of impurity localisation in quantum wells of finite width, we intoduce a correction (scale) factor, γ, independent of the number of the level, into the coefficients β_i: $\beta_i = 2\gamma/[(i - 1/2)a$ (level energies $E_i = -q^2\gamma[2(i - 1/2)^2\varepsilon a]^{-1}$). In the 2D case, $\gamma = 1$. The use of the scale factor γ is formally equivalent to variations in mass in the problem of a two-dimensional hydrogen atom. Equating the probability of spontaneous acoustic phonon emission in the $2p_0$–1s transition to the recombination rate, we obtain

$$v_r = \frac{16E_D^2 q^{10} m^3 \gamma^3}{9\pi\hbar^9 \varepsilon^5 s^4 \rho_{cr}} J(\gamma,\chi), \tag{10}$$

where

$$J(\gamma,\chi) = \int_0^\chi \frac{|F(8\gamma x/3a)|^2(\chi^2 - x^2)^2 \mathrm{d}x}{(1 + \chi^2 - x^2)^5};$$

$$F(q_z) = \int_{-\infty}^{+\infty} |\psi_1(z)|^2 \exp(-\mathrm{i}q_z z)\mathrm{d}z; \text{ and } \chi = \frac{2q^2}{3\varepsilon\hbar s}.$$

For GaAs, $\chi \approx 20.4 \gg 1$, so in two dimensions [$|F(q_z)| = 1$] the asymptotic expansion $J(\gamma = 1,\chi) \approx \chi^{-1}/24$ ensures a good approximation. The recombination rate strongly decreases with increasing quantum well thickness, which is caused by two factors, acting in the same direction: the dependence of $J(\gamma,\chi)$ on thickness and the factor γ^3 in Eqn (10) (with increasing quantum well thickness, the binding energy of the impurity and, hence, γ decrease).

As an example, consider a GaAs layer in an infinitely deep quantum well approximation. In the 2D case (at zero thickness), $v_r \approx 8 \times 10^{10}$ s^{-1}; at a quantum well thickness of 7 nm, the recombination rate drops to $\sim 3 \times 10^6$ s^{-1}. In the latter instance, in our estimates we used $\gamma \approx 0.43$ ($\gamma = |E_1|/E_i^{(2D)} = |E_1|\varepsilon^2\hbar^2/(2mq^4)$, $|E_1| \approx 10$ meV), which roughly corresponds to the characteristics of donors in $In_{0.17}Ga_{0.83}As$ quantum wells of the same thickness in experiments dealing with the photoexcitation of GaAs/InGaAs heterostructures [9]. The experimentally measured recombination rate of $\sim 10^8$ s^{-1}, exceeding the above estimate, is presumable due to the relaxation of the hot electrons from the distribution function tail through optical phonon emission [9].

In the 2D case, for n-GaAs we have $v_{th}/v_r \approx 1.2$ at $N_{2D} = 5 \times 10^{10}$ cm^{-2} and $T_e = 40$ K; at a temperature of 20 K, we have $v_{th}/v_r \approx 0.7$. At a donor concentration $N_{2D} = 5 \times 10^{11}$ cm^{-2} in n-Si, $v_{th}/v_r \approx 3.1$ at $T_e = 40$ K and about 1.7 at a temperature of 20 K.

Summarising the above, we see that, the gain is influenced by several factors in going from the 3D case to a quasi-two-dimensional system. First, a negative role is played by the increase in ground state recombination rate, which is attributable to wave function localisation in the layer and the corresponding wave function delocalisation in momentum space [14]. A second factor associated with impurity localisation in the quantum layer is the increase in the impurity binding energy. On the one hand, this leads to a reduction in the gain cross section for impurity–band transitions; on the other, this reduces the loss due to the absorption by free charge carriers. Yet another consequence of localisation is an increase in the absorption cross section at the pump frequency, as follows from comparison of Eqns (7) and (8). The total balance of the positive and negative factors should take into account the internal loss. With allowance for losses, quantisation in the layer improves the relationship between the gain and absorption, as shown below.

3. Internal loss and gain

Let us compare the gain coefficient for a working transition to the internal loss. In the conditions under consideration, the internal loss is due to the absorption by continuum electrons. To evaluate the cross section of this absorption, we use the Drude–Lorentz classical relation [19]

$$\sigma_D = \frac{4\pi q^2 \nu}{mc\sqrt{\varepsilon}\,(\omega^2 + \nu^2)}, \tag{11}$$

where ν is the collision frequency. Clearly, at a high doping level, scattering by charged centres prevails and we have in the Conwell–Weisskopf model [20]

$$\nu = \frac{\pi q^4 N_I}{\sqrt{2m}\,\varepsilon^2 E^{3/2}} \ln\left(1 + \frac{\varepsilon^2 E^2}{q^4 N_I^{2/3}}\right), \tag{12}$$

where $E = k_B T_e$ is the electron energy and $N_I = N^+$ ($K = 0$) is the number of ionised centres. Note that a similar result is provided by the Brooks–Herring formula [21].

With the above relations, we can compare the gain coefficient α at the red limit of the photoeffect, $\omega_{red} = E_i/\hbar$, to the absorption coefficient $\beta = \sigma_D n_{3D}$. Analytical estimates can be obtained in the $v_I \gg v_r$ limit, which corresponds to the complete ionisation of impurities: $N^+ \approx n$. This will make it possible to answer the question of whether the gain can in principle exceed the loss. In the 3D case, we have

$$\frac{\alpha}{\beta} = \frac{G_0}{\eta G}\left(1 + \frac{\nu^2}{\omega_{red}^2}\right), \tag{13}$$

where $G_0 = 2^7\pi^{3/2}/3e^4 \approx 4.35$; e is the base of the natural logarithms; and G is the logarithm in (12). It follows from (13) that the gain to absorption ratio decreases logarithmically with increasing temperature. Note also that, in the limiting case under consideration, the ratio in (13) is only related to the effective mass through the frequency factor ν/ω_{red}.

As an example, consider GaAs with shallow donors in the high excitation intensity limit: $v_I \gg v_r$. At a concentration $n_{3D} \approx N^+ \approx N = 10^{16}$ cm^{-3}, the temperature T_e at which the gain is twice as high as the absorption is 80 K. At this temperature, the gain cross section at the red limit of the photoeffect ($\hbar\omega_{red} \approx 5.8$ meV) is $\sigma = \alpha/N \approx 2 \times 10^{-14}$ cm^2 [$\alpha \approx 200$ cm^{-1}, $\sigma_I(\omega_{red}) \approx 6.2 \times 10^{-14}$ cm^2, $f_{3D} = 0.17$], whereas the absorption cross section is $\sigma_D \approx 10^{-14}$ cm^2 ($\nu \approx 1.8 \times 10^{12}$ s^{-1}).

At a realistic ratio $v_I/v_r = 2$ (CO_2 laser pump power near 0.2 MW cm^{-2}) and $T_e = 40$ K, the gain coefficient α is $\sim$120 cm^{-1} ($\sigma \approx 1.2 \times 10^{-14}$ cm^2) and the Drude absorption β is $\sim$70 cm^{-1} ($\sigma_D \approx 0.7 \times 10^{-14}$ cm^2). For comparison, Fig. 2 shows the gain cross section in the case of complete ionisation ($v_I \gg v_r$) at the same electron temperature. The Drude absorption cross section in Fig. 2 was estimated using classical and quantum approaches [21].

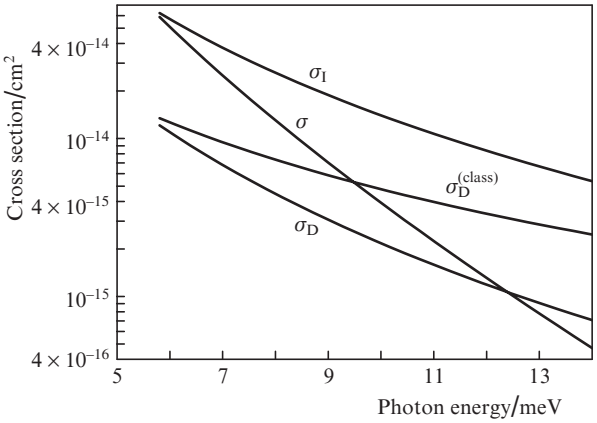

Figure 2. Photoionisation cross section σ_I of shallow donors in GaAs, gain cross section σ for impurity–band transitions at $v_I \gg v_r$ and Drude absorption cross section in classical ($\sigma_D^{(class)}$) and quantum (σ_D) approaches vs. photon energy. The electron temperature is 40 K, the dopant concentration is 10^{16} cm^{-3}, and the scattering frequency in the Drude classical model is 2.5×10^{12} s^{-1}.

Consider how the relationship between the gain and absorption will change in going from a 3D to a 2D system. The classical formula (11) for the Drude absorption cross section is valid as well in the two-dimensional case, but with corrections for the scattering frequency ν. To calculate this frequency, we take advantage of the Conwell–Weisskopf model [22]. We will use the minimum scattering angle, determined by the maximum impact parameter b_{max}. The parameter b_{max} is, in turn, equal to half the average spacing between the ions, which is determined by their concentration. We assume that scattering occurs in the field of one ion. In the two-dimensional case, we have

$$b_{max} = \frac{1}{2\sqrt{N_I^{(2D)}}},$$

where $N_I^{(2D)}$ is the number of ions per unit area. Using Conwell and Weisskopf's approach [22] to the problem of scattering by a two-dimensional Coulomb potential [23], it is easy to find the total transport scattering cross section:

$$\sigma_{sc}^{(2D)} = \frac{2q^2}{\varepsilon E} \arctan\left(\frac{\varepsilon E}{q^2\sqrt{N_I^{(2D)}}}\right), \qquad (14)$$

where E is the incident-electron energy. Accordingly, the scattering frequency is

$$\nu = N_I^{(2D)} v \sigma_{sc}^{(2D)}, \qquad (15)$$

where v is the mean electron velocity. In our estimates, we take $E = k_B T_e$ and $v = \sqrt{2E/m}$. At the frequency corresponding to the red limit of the photoeffect, the ratio of the gain coefficient α to the Drude absorption coefficient β in the limiting case is

$$\frac{\alpha}{\beta} = \frac{2^{5/2}\pi^2 q^2 m^{1/2}}{e^2 \varepsilon \hbar \eta (k_B T_e)^{1/2} \arctan[\varepsilon k_B T_e/(q^2 n_{2D}^{1/2})]}\left(1 + \frac{\nu^2}{\omega_{red}^2}\right). \qquad (16)$$

Note that, in contrast to (13), (16) has an additional dependence on effective mass, and the dependence on temperature and permittivity is stronger.

As an example, consider a shallow donor-doped 2D GaAs layer at $T_e = 80$ K and $n_{2D} \approx N_I^{(2D)} = 5 \times 10^{10}$ cm^{-2}. At the red limit of the photoeffect ($\hbar\omega_{red} \approx 23.2$ meV), the gain cross section is then $\sigma \approx 1.1 \times 10^{-14}$ cm^2 [$\sigma_I(\omega_{red}) \approx 2.2 \times 10^{-14}$ cm^2, $f_{2D} \approx 0.26$] and the absorption cross section is $\sigma_D \approx 1.4 \times 10^{-15}$ cm^2 ($\nu \approx 3.8 \times 10^{12}$ s^{-1}). It can be seen that the gain cross section is smaller than that in bulk GaAs, but its ratio to the absorption cross section is markedly greater.

4. Discussion

Let us discuss the above results, comparing the 3D and 2D cases. Note, first of all, the conclusion drawn: in both cases, the gain may exceed the absorption at moderate electron gas temperatures. Since the electron temperature is a key parameter, the ability to minimise heating is an important issue, which should be resolved by selecting the semiconductor, pump wavelength etc.

Let us compare the two dimensionalities, considering each factor influencing the gain and absorption. In going from the 3D to 2D case, the frequency corresponding to the red limit of the photoeffect increases four times and the photoionisation cross section at this frequency decreases by a factor of $2^6/3e^2 \approx 3$. Accordingly, the Drude absorption cross section (11) decreases by about a factor 16 on account of the $\omega^2 + \nu^2 \approx \omega^2$ term in the denominator. These two factors have the strongest effect on the gain and absorption when the dimensionality of the system changes. The Drude absorption is also influenced by changes in scattering frequency. The collision frequencies for the two dimensionalities of the electron gas are, however, difficult to compare because the frequency depends on impurity concentration, which has different dimensions in the 2D and 3D cases. For the same reason, other concentration-dependent factors are also difficult to analyse.

Clearly, the contribution of the Drude absorption to the losses prevails. At the same time, we believe that the classical formula (11) gives an overestimated cross section. It is seen from Fig. 2 that the quantum formula [21] gives a smaller cross section than does (11), even though, in deriving it, the shielding of the Coulomb potential of impurities was neglected. A considerable number of excited electrons should be present in the band of quasi-localised states, D, which is equivalent to the neutralisation or strong shielding of impurity ions. In our calculations, we assumed that those electrons are in a continuum and contribute to the Drude absorption, possessing appropriate mobility. This approach overestimates

the number of ionised impurities acting as scattering centres. On the other hand, note that the D–GS working optical transitions (Fig. 1) lie in a longer wavelength range than do the band–impurity (CS–GS) transitions in the one-centre approximation used. This should lead to an increase in both the Drude absorption and the cross sections of the working transitions. Taking into account these circumstances requires more complex models, beyond the one-centre approximation.

The gain conditions (13) and (16) are rather a starting point for analysing the feasibility of gain in a real situation, because they were derived in the idealised limit $v_I \gg v_r$. In the $v_I/v_r \to \infty$ limit, gain conditions are independent of the recombination rate v_r, which in turn depends on material parameters and pumping conditions. In the model under consideration, the recombination rate in both a bulk semiconductor and quantum wells is proportional to m^3 [see (9) and (10)]. For comparison, the capture rate in excited states of impurities in bulk semiconductors is proportional to $m^{5/2}$ [15]. The relaxation and recombination processes are also influenced significantly by Umklapp electron–phonon scattering, which is possible for multivalley wave functions of impurity states, as e.g. in n-Si, where Umklapp processes considerably increase the recombination rate.

Another important parameter influencing the relationship between the gain and loss is the order of degeneracy of band extrema, η. We saw above that, in the case of n-Si, excitation powers necessary for population inversion on CS–GS transitions are too high, which is caused by both the high recombination rate and the degeneracy of the conduction band minima ($\eta = 6$). The order of degeneracy can be reduced to $\eta = 2$ by uniaxial deformation of bulk silicon, e.g. in the [100] direction, or in deformed silicon layers grown on virtual (100) GeSi substrates. A decrease in the order of degeneracy will influence the distribution function, in particular through the reduction in electron relaxation rate due to the decrease in the density of states and the fact that the intervalley f-phonons are not involved in scattering processes. As a rough approximation, we think that the pump power necessary for population inversion can be reduced by about a factor of 3 as a result of the deformation splitting of the valleys. Note also that, in the case of n-Si, a four-level excitation scheme may be possible, where the lower working state is one of the excited levels resulting from the splitting of the 1s level by the short-range potential of an impurity.

It is of interest to discuss the effect of the chemical shift on the relationship between the gain and absorption. In our estimates, we use results reported by Chaudhuri [24], who examined the effect of the chemical shift on the photoionisation cross section using the quantum defect method. Bloch waves without Coulomb perturbation were used as wave functions of the continuum. We modelled the effect of the chemical shift using a hypothetical example with parameters of n-GaAs. As the donor binding energy was increased by a factor of 1.5, the maximum photoionisation cross section dropped by about a factor of 2.5. Assuming that the Drude absorption is proportional to ω^{-2}, we find that, at this energy shift, it will decrease by a factor of $1.5^2 = 2.25$. Thus, to a rough approximation the chemical shift does not improve the σ_I/σ_D ratio. It should, however, be kept in mind that the gain is influenced considerably by the recombination rate v_r, which should decrease with decreasing ground state energy, thereby having a beneficial effect on the gain.

Note an experimental study by Zakhar'in et al. [7], who carried out spectral identification of impurity–band transitions for interband optical excitation of n-GaAs with an impurity concentration $N_D - N_A = 5 \times 10^{15}$ and 8×10^{16} cm^{-3}. These concentrations are, respectively, below and above the critical concentration for the Mott transition (1.6×10^{16} cm^{-3}) [25]. It is worth noting that a considerable fraction of the power of the observed terahertz luminescence is emitted in the spectral region corresponding to impurity–band transitions, rather than intracentre ones. In Fig. 1, this spectral region includes the CS–GS transitions, which are formally equivalent to transitions from a continuum of 'isolated' coulomb centres. The question of from which states (D or C) impurity–band transitions will occur depends on particular conditions and should be examined separately.

There is particular interest in experiments on the intraband optical excitation of impurities using the scheme under discussion. Such experiments were performed with multiperiod selectively doped quantum-well n-type GaAs/InGaAs heterostructures [9]. The quantum well thickness was 7 nm, the indium content of the quantum wells was 17%, and the effective mass was $m \approx 0.06m_0$. The structures were doped into the quantum wells and/or barriers. In some of the heterostructures, the barrier regions contained an $In_{0.05}Ga_{0.95}As$ shallow quantum well 14 nm in thickness. In the case of doping in the centre of a deep well, the calculated donor binding energy is ~10 meV. The heterostructures were excited on their end faces by a CO_2 laser ($\hbar\Omega = 117$ meV). For some of the heterostructures, the terahertz luminescence intensity measured on their end faces as a function of pump power showed superlinear behaviour, indicating that the emission was amplified. Figure 3 shows such a curve for a delta-doped deep quantum well $In_{0.17}Ga_{0.83}As$ heterostructure. Roughly estimated using filters, the spectral range of luminescence of the heterostructures lies at photon energies from 12 to 14 meV, which corresponds to impurity–band transitions.

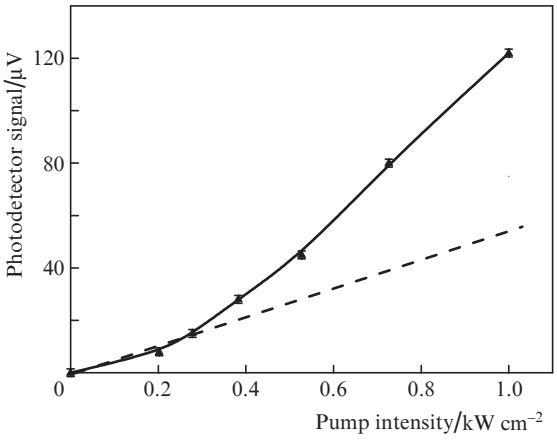

Figure 3. Spontaneous emission power as a function of CO_2 laser pump intensity for a delta-doped quantum well GaAs/$In_{0.17}Ga_{0.83}As$ structure pumped on its end face (solid line). The dashed line shows extrapolation of the linear portion [9].

The accumulation of photoexcited electrons after their relaxation through the emission of optical phonons should occur near the bottom of the first subband and in excited donor states. This follows from comparison of three key energies: optical phonon energy (36 meV), pump photon energy (117 meV) and donor binding energy (10 meV). It follows from the relationship between these values that the fast stage

of photoexcited electron relaxation should terminate after threefold emission of optical phonons, with a final electron energy near the minimum of the lower subband. Thus, according to our estimates the hot electron temperature in the lower subband should not exceed 40 K, which ensures favourable conditions for gain on impurity–band optical transitions. The gain coefficient in the frequency range 3–3.4 THz was measured to be ~100 cm^{-1}. Note that quantum well heterostructures offer an additional advantage associated with the possibility of increasing the photoexcitation cross section of impurities by using polarisation in which the electric field of the wave is normal to the plane of the quantum wells (TM polarisation). At a lateral polarisation, in the 2D layer approximation, the donor photoionisation cross section in GaAs is $\sim 5 \times 10^{-16}$ cm^2 at $\hbar\Omega = 117$ meV. For the TM polarisation, the donor photoionisation cross section is comparable to the photoionisation cross section of the quantum wells or intersubband transitions. This cross section can be maximised by adjusting the quantum well depth. In $In_{0.17}Ga_{0.83}As/GaAs$ quantum wells [9], whose parameters are not optimal from the viewpoint of photoionisation, its cross section is $\sim 10^{-14}$ cm^2 at $\hbar\Omega = 117$ meV. In such structures, gain effects were found at a rather low pump power density (~1 kW cm^{-2}).

When electrical pumping is used in order to reduce electron heating, vertical transport can be employed in quantum well heterostructures. The principle of producing an inverted distribution considered in Ref. [10] can be illustrated by Fig. 4, which shows the electron wave functions of 2D subbands in a system of tunnelling-coupled quantum wells of a cascade period. The narrow quantum well is selectively doped with donors or acceptors. The other parameters of the structure should be adjusted so that the impurity GS level (lower resonance state under subband 3) nearly coincides with the bottom of subband 2. At the working voltage, the wave function of the ground state of a Coulomb centre (shown by a black line) penetrates the wide quantum well of the cascade, which can be accounted for by the hybridisation of this state with states of subband 2. In the case of fast electron relaxation from subband 2 to subband 1, accompanied by the emission of an optical phonon on the 3-CS–GS optical transition (Fig. 4), population inversion may result. Thus, owing to the resonance tunnelling effect, the optical pumping of population inversion on a CS–GS transition can be replaced by electrical pumping. It should be emphasised that, with such a scheme, the ionisation rate of a Coulomb centre may be rather high (up to $\sim 10^{12}$ s^{-1} [10]), considerably exceeding the recombination rate.

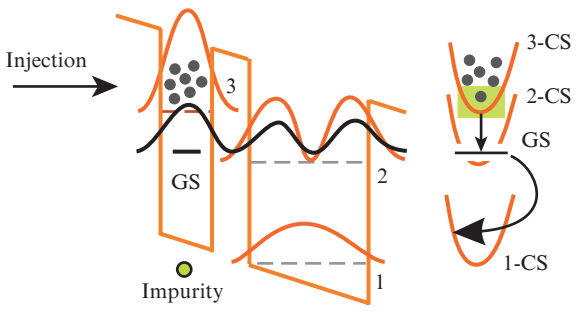

Figure 4. Schematic of a cascade laser based on impurity–band optical transitions in quantum wells. The wave functions of the subbands are shown by grey lines. GS is the ground state level of the impurity. The corresponding wave function is shown by a black line. Right side: optical (vertical arrow) and tunnelling (curved arrow) transitions accompanied by the emission of optical phonons. CS = subband continuums, numbered like the corresponding subbands.

Electrical pumping based on quantum cascade heterostructures has its own specific features, differentiating it from optical pumping. First, the operation of such a scheme in the case of vertical transport implies a relatively fast depopulation of the impurity ground state upon electron tunnelling to a wide quantum well (Fig. 4), which requires mixing of the wave function of subband 2 to the ground state (hybridisation effect). The hybridisation effect reduces the contribution of subband 3 to the wave function of the ground state, thus reducing the matrix elements of impurity–band optical transitions [10]. Thus, the matrix elements of optical transitions involving resonance states will be smaller than those for truly localised states in the optical pumping scheme considered above.

Another distinctive feature of the electrical pumping scheme also has an adverse effect on the gain. It is related to the fact that, under resonance tunnelling conditions, the working subband (subband 3 in Fig. 4) combines with the lower subband of the preceding cascade to form an injection doublet [10] (not shown in Fig. 4). As a result, injected electrons become distributed over the two subbands of the doublet and, accordingly, their occupation numbers decrease by a factor of 2.

According to preliminary calculations, the gain on working impurity–band transitions in n-GaAs/AlGaAs, n-Si/SiGe(111) and p-Ge/GeSi quantum cascade heterostructures is comparable to the Drude loss (to within the accuracy of the models used). The drastic distinction of quantum cascade schemes from optical pumping schemes is caused primarily by the above two negative factors inherent in electrical pumping. Further research into quantum cascade schemes should include more detailed theoretical models and approaches and experimental studies. The potential of the quantum cascade amplification scheme based on impurity–band transitions depends on the ability to reduce electron heating and optimise the scheme.

The main conclusions of this study are as follows: The amplification scheme based on impurity–band optical transitions has been shown to be viable, but only at relatively low electron (hole) temperatures. We have presented analytical estimates of gain and absorption cross sections in the two- and three-dimensional cases, which have been used to analyse the effect of material parameters and electron temperature on conditions under which gain is possible. The amplification scheme based on impurity–band transitions is quite attractive under optical pumping. In the above example of a quantum cascade amplification scheme, the absorption proved to be comparable to the gain (to within the accuracy of the models used). The deterioration of the relationship between the gain and absorption is related to the specifics of the electrical pumping scheme in quantum cascade heterostructures: the decrease in the dipole matrix elements of their working optical transitions because of the hybridisation effect and the decrease in occupation numbers in the continuum of the working subband because of the electron distribution over the subbands of the injection doublet. Further research, primarily experimental work, is needed to ascertain whether amplification in quantum cascade schemes is possible.

Acknowledgements. This work was supported by the Russian Foundation for Basic Research (Grant Nos 12-02-01231 and 13-02-12108 ofi_m) and the Presidium of the Russian Academy of Sciences (Fundamental Issues in the Technology of Nanostructures and Nanomaterials Programme).

References

1. Williams B.S. *Nat. Photonics*, **1**, 517 (2007).
2. Pavlov S.G., Zhukavin R.Kh., Shastin V.N., Hübers H.-W. *Phys. Status Solidi (B)*, **250**, 9 (2013).
3. Adam T.N., Troeger R.T., Ray S.K., Lv P.-C., Kolodzey J. *Appl. Phys. Lett*., **83**, 1713 (2003).
4. Lv P.-C., Troeger R.T., Kim S., Ray S.K., Goossen K.W., Kolodzey J., Yassievich I.N., Odnoblyudov M.A., Kagan M.S. *Appl. Phys. Lett*., **85**, 3660 (2004).
5. Lv P.-C., Troeger R.T., Adam T.N., Kim S., Kolodzey J., Yassievich I.N., Odnoblyudov M.A., Kagan M.S. *Appl. Phys. Lett*., **85**, 22 (2004).
6. Shalygin V.A., Vorobjev L.E., Firsov D.A., Panevin V.Yu., Sofronov A.N., Melentyev G.A., Antonov A.V., Gavrilenko V.I., Andrianov A.V., Zakharyin A.O., Suihkonen S., Törma P.T., Ali M., Lipsanen H. *J. Appl. Phys*., **106**, 123523 (2009).
7. Zakhar'in A.O., Andrianov A.V., Egorov A.Yu., Zinov'ev N.N. *Appl. Phys. Lett*., **96**, 211118 (2010).
8. Hübers H.-W., Pavlov S.G., Shastin V.N. *Semicond. Sci. Technol*., **20**, S211 (2005).
9. Bekin N.A., Zhukavin R.Kh., Kovalevsky K.A., Pavlov S.G., Zvonkov B.N., Uskova E.A., Shastin V.N. *Fiz. Tekh. Poluprovodn*., **39**, 76 (2005) [*Semiconductors*, **39**, 67 (2005)].
10. Bekin N.A., Shastin V.N. *Fiz. Tekh. Poluprovodn*., **42**, 622 (2008) [*Semiconductors*, **42**, 608 (2008)].
11. Bekin N.A., Pavlov S.G. *Physica B*, **404** (23-24), 4716 (2009).
12. Basov N.G., Vul B.M., Popov Yu.M. *Zh. Eksp. Teor. Fiz*., **37**, 587 (1959).
13. Altermatt P.P., Schenk A., Heiser G. *J. Appl. Phys*., **100**, 113714 (2006).
14. Abakumov V.N., Perel V.I., Yassievich I.N. *Nonradiative Recombination in Semiconductors* (Amsterdam: North-Holland, 1991; St. Petersburg: Nauchno-Issled. Inst. Yadernoi Fiziki, 1997).
15. Abakumov V.N., Perel V.I., Yassievich I.N. *Zh. Eksp. Teor. Fiz*., **72**, 674 (1977) [*Sov. Phys. JETP*, **45**, 354 (1977)].
16. Thomas G.A., Capizzi M., DeRosa F., Bhatt R.N., Rice T.M. *Phys. Rev. B*, **23**, 5472 (1981).
17. Sclar N. *Prog. Quantum Electron*., **9**, 149 (1984).
18. Yang X.L., Guo S.H., Chan F.T., Wong K.W., Ching W.Y. *Phys. Rev. A*, **43**, 1186 (1991).
19. Yu P.Y., Cardona M. (Eds) *Fundamentals of Semiconductors: Physics and Materials* (Berlin: Springer, 2010, 4th ed.; Moscow: Fizmatlit, 2002).
20. Conwell E.M. *High Field Transport in Semiconductors* (New York: Academic, 1967; Moscow: Mir, 1970).
21. Seeger K. *Semiconductor Physics* (Vienna: Springer, 1973; Moscow: Mir, 1977).
22. Conwell E., Weisskopf V.F. *Phys. Rev*., **77**, 388 (1950).
23. Stern F., Howard W.E. *Phys. Rev*., **163**, 816 (1967).
24. Chaudhuri S. *Phys. Rev. B*, **26**, 6593 (1982).
25. Benzaquen M., Walsh D., Mazuruk K. *Phys. Rev. B*, **36**, 4748 (1987).